Journal of Biotechnology 200 (2015) 38–43

Contents lists available at ScienceDirect

Journal of Biotechnology

journal homepage: www.elsevier.com/locate/jbiotec

Metabolic reconfigurations aimed at the detoxification of a multi-metal stress in *Pseudomonas fluorescens*: Implications for the bioremediation of metal pollutants

Azhar Alhasawi, Jacob Costanzi, Christopher Auger, Nishma D. Appanna, Vasu D. Appanna*

Faculty of Science and Engineering, Laurentian University, Sudbury, ON, Canada

ARTICLE INFO

Article history:
Received 10 October 2014
Received in revised form 29 January 2015
Accepted 31 January 2015
Available online 24 February 2015

Keywords:
Oxalate
ATP
Alternate TCA cycle
Bioremediation
Metal toxicity

ABSTRACT

Although the ability of microbial systems to adapt to the toxic challenge posed by numerous metal pollutants individually has been well documented, there is little detailed information on how bacteria survive in a multiple-metal environment. Here we describe the metabolic reconfiguration invoked by the soil microbe *Pseudomonas fluorescens* in a medium with millimolar amounts of aluminum (Al), iron (Fe), gallium (Ga), calcium (Ca), and zinc (Zn). While enzymes involved in the production of NADH were decreased, there was a marked increase in enzymatic activities dedicated to NADPH formation. A modified tricarboxylic acid (TCA) cycle coupled to an alternate glyoxylate shunt mediated the synthesis of adenosine triphosphate (ATP) with the concomitant generation of oxalate. This dicarboxylic acid was a key ingredient in the sequestration of the metals that were detoxified as a lipid complex. It appears that the microbe favors this strategy as opposed to a detoxification process aimed at each metal separately. These findings have interesting implications for bioremediation technologies.

1. Introduction

Metal pollution is an ongoing global problem as it affects all organisms. Although in trace amounts some metals are known to be essential, in elevated concentrations all metals are deleterious to living systems (Rajapaksha et al., 2004). The toxic properties of metals are attributed to their ability to interfere with critical biological processes. While aluminum (Al) perturbs iron metabolism, a key component of aerobic respiration, zinc (Zn) an essential micronutrient, is known to trigger the production of reactive oxygen species (ROS) (Lemire et al., 2010a; Alhasawi et al., 2014). Most organisms succumb to the noxious influence of metal toxicity. However, numerous microorganisms, due to their malleable genetic features, have evolved intricate mechanisms to survive in extreme environments (Wingfield et al., 2011).

Volatilization, intracellular sequestration, active efflux systems and precipitation are some of the strategies microbes invoke to proliferate in metal polluted surroundings (Clemens, 2001; Hall, 2002). Mercury toxicity is circumvented via its volatilization while lead is immobilized as insoluble sulphide and phosphate derivatives (Appanna and Hamel, 1996; Song and Van Heyst, 2005; Adeyemi, 2010). The up-regulation of a CO_2-fixing system has been demonstrated to be key to the survival of *P. fluorescens* in elevated Ca as it aids in the elimination of this divalent metal as $CaCO_3$ (Anderson et al., 1992). Metalothioneins contribute to the intracellular sequestration of Zn and cadmium (Blindauer et al., 2002). Some tellurium (Te)-resistant bacteria devise an elaborate biochemical system that enables the biotransformation of this metal into innocuous moieties and generate anti-oxidants to quell Te-induced oxidative stress (Reinoso et al., 2012, 2013).

Although the mechanisms involved in the detoxification of a single metal toxicant have been well-documented, there has been relatively scant information on the strategies utilized to combat an environment with numerous toxic metals, a situation common in nature (Appanna and St Pierre, 1996). In this study we have evaluated the metabolic networks that allow the nutritionally-versatile microbe, *Pseudomonas fluorescens* to tolerate millimolar amounts of Al, Zn, Fe, Ca and Ga. We have previously demonstrated the extracellular sequestration of the metals as a lipid residue (Appanna and St Pierre, 1996). Here we show that instead of invoking disparate detoxification pathways aimed at each metal, the microbe immobilizes the five toxicants as an insoluble oxalate-rich precipitate.

* Corresponding author. Tel.: +1 705 675 1151x2112.
E-mail address: vappanna@laurentian.ca (V.D. Appanna).

http://dx.doi.org/10.1016/j.jbiotec.2015.01.029
0168-1656/

The metabolic networks designed to generate NADPH are enhanced while activities of enzymes responsible for NADH production are reduced. Furthermore, oxalate and ATP synthesis are promoted by an alternate TCA cycle and the glyoxylate shunt. The significance of this detoxification strategy in bioremediation technology is also discussed.

2. Methods

2.1. Bacterial culture and isolation of cellular fractions

Pseudomonas fluorescens (ATCC 13525) was obtained from the American Type Culture Collection. It was maintained and grown in mineral medium containing Na_2HPO_4 (0.06 g); KH_2PO_4 (0.03 g); NH4Cl (0.8 g); $MgSO_4{\cdot}7H_2O$ (0.2 g), and citric acid (4 g) per liter of deionized water. Citrate (19 mM) was utilized as a carbon source, and the five metals complexed to citrate were $AlCl_3$ (5 mM), $FeCl_3$ (5 mM), Zn $(NO_3)_2$ (3 mM), $CaCl_2$ (2 mM) and $Ga(NO_3)_3$ (1 mM). The pH was adjusted to 6.8 with 2N NaOH. Trace elements were present in concentrations as described previously (Anderson et al., 1992). The medium was inoculated with 1 ml of stationary-phase cells grown in a multiple-metal medium in an aerated gyratory water bath shaker, model 76 (New Brunswick Scientific, Enfield, CT) at 26 °C and 140 rpm. The bacterial cells were harvested at similar growth phases (24 h for control and 27 h for stressed media) (Appanna and St Pierre, 1996). Following centrifugation at 10,000 × *g* for 15 min at 4 °C, cells were washed with 0.85% NaCl and re-suspended in cell storage buffer (CSB: 50 mM Tris-HCl, 5 mM $MgCl_2$, 1 mM phenylmethylsulfonylfluoride (PMSF) and 1 mM dithiothreitol (DTT), pH 7.3). The soluble cell-free extract (CFE) and membrane CFE were obtained by sonication followed by centrifugation at 180,000 × *g* for 3 h at 4 °C (Singh et al., 2005). Purity was assessed by the activity of malic enzyme for soluble CFE and complex I for membrane CFE. The protein content was measured by the Bradford assay. These CFE fractions were kept at 4 °C for up to 5 days and various enzymatic activities were performed (Bradford, 1976).

2.2. Metabolite analyses

The relative levels of various metabolites from the spent fluid and soluble CFE in control and metal-stressed cultures were determined by high performance liquid chromatography (HPLC). Enzymatic activity was immediately quenched at the desired time by boiling the soluble CFE for ten min to denature and precipitate proteins. These were then centrifuged out of solution at 15,000 × *g* for 10 min. The supernatant was filtered and injected into an Alliance HPLC equipped with C18 reverse-phase column at a flow rate of 0.7 ml min^{-1}. The samples were diluted 10-fold using Milli-Q water and run in mobile phase containing 20 mM KH_2PO_4, pH 2.9 prepared in Milli-Q water. For the measurement of NAD(P)H, the mobile phase used was 20 mM KH_2PO_4, pH 7.0 with 5% acetonitrile (Singh et al., 2007). The samples were loaded into the HPLC (Waters 2695 separation module) and EMPOWER software (Milford, MA) was used for the automatic injection protocol. Metabolites and nucleotides were detected by using a Waters model 2487 UV–vis dual wavelength detector operating at 210 and 254 nm, respectively. Peaks were identified by comparing to known standards and by spiking the samples with known standard solutions (Lemire et al., 2010b). Oxalate was measured in the gelatinous pellet after suspension in H_2O and following acidification to pH 2.0 with HCl. The production of ATP was monitored in the lyzed control and stressed bacteria following the addition of 5 mM KCN, 2 mM citrate and 0.5 mM ADP for 30 min to demonstrate that the metal-treated microbes were utilizing substrate level phosphorylation to generate energy. To verify how citrate was providing ATP via the glyoxylate shunt, the soluble CFE from control and multiple metal-treated cells was incubated with 2 mM glyoxylate, 2 mM succinate and 0.5 mM ADP for 30 min and the reaction was monitored by HPLC. Experiments where isocitrate (2 mM) was substituted for glyoxylate and succinate were also conducted.

2.3. Monitoring enzymatic activity

BN-PAGE was performed as per the protocol described (Auger et al., 2012). For these assays, a 4–16% gradient gel was cast and the protein (4 mg/ml) was prepared in blue native buffer (400 mM 6-aminohexanoic acid, 50 mM bis–tris; pH 7.0). A final concentration of 1% dodecyl-β-maltoside was added to the membrane fractions to solubilize membrane-bound proteins. In order to ensure optimal protein separation, protein samples were loaded into each well of the native gel (10–60 μg) and electrophoresed at 4 °C under native conditions at 80 V and 15 mA for proper stacking followed by 150 V and 25 mA in the resolving gel for the migration of the protein until it traveled halfway through the gel. At this point, blue cathode buffer (50 mM tricine, 15 mM bis–tris, 0.02% (w/v) Coomassie G-250; pH 7.0) was replaced by a colorless cathode buffer (50 mM tricine, 15 mM bis–tris, pH 7.0) to improve the detection of the protein bands. After which, electrophoresis was completed at 300 V and 25 mA. For 15 min following the electrophoresis, the gel was incubated in reaction buffer (25 mM Tris–HCl, 5 mM $MgCl_2$, pH 7.4) prior to performing in-gel activity assays. These were completed by using a reaction mixture containing reaction buffer, substrates and cofactors. In-gel activity was established using iodonitrotetrazolium chloride (INT) which precipitates as formazan when reduced, coupled to phenazine methosulfate (PMS) or dichloroindophenol (DCIP) as described (Han et al., 2013). Destaining solution (40% methanol and 10% glacial acetic acid) was used to stop the reactions. NAD and NADP-dependent isocitrate dehydrogenase (ICDH-NAD and ICDH NADP, respectively), alpha ketoglutarate dehydrogenase (αKGDH), isocitrate lyase (ICL), acylating glyoxylate dehydrogenase (AGODH) and malic enzyme (ME) activities were visualized as described (Anderson et al., 1992; Singh et al., 2005; Auger et al., 2012; Hamel and Appanna, 2001). Complex I was measured with 5 mM KCN, 0.5 mM NADH and INT. Cytochrome C oxidase (complex IV) activity was deduced with the utilization of equilibration buffer supplemented with 10 mg/ml of diaminobenzidine, 10 mg/ml cytochrome C and 562.5 mg/ml of sucrose (Auger et al., 2012). Spectrophotometric data for ICDH-NAD(P) was obtained by incubating 1 mg of membrane CFE from control and metal-treated cells with 2 mM isocitrate and 0.5 mM NAD(P) for 1 min. A similar mixture was used for MDH, but isocitrate was replaced with malate. For malic enzyme, NAD was replaced by NADP. For acylating glyoxylate dehydrogenase, 1 mM glyoxylate, 0.1 mM CoA and 0.1 mM NADP were used in the reaction mixture for 1 min. The production of reduced nicotinamides (NAD(P)H) was monitored at 340 nm. For pyruvate carboxylase (PC) analysis, the membrane CFE was given 2 mM pyruvate, 0.5 mM ATP, 0.5 mM HCO_3^-, 10 units of MDH and 0.5 mM NADH. The disappearance of NADH was monitored at 340 nm over the course of 1 min. Negative controls were performed without the substrates or cofactors (Auger et al., 2012).

2.4. Statistical analysis

Data were expressed as means ± standard deviations. Statistical correlations of the data were checked for significance using the Student *t*-test ($p \leq 0.05$). All experiments were performed at least twice and in triplicate.

3. Results and discussion

Pseudomonas fluorescens has been shown to survive a medium with millimolar concentrations of Al, Zn, Fe, Ca and Ga (Appanna and St Pierre, 1996). The metals are predominantly immobilized as an insoluble pellet that had a characteristic brown-gelatinous appearance (Fig. 1A). Most of the toxic metals have previously been shown to be localized in this pellet (Appanna and St Pierre, 1996). In an effort to elucidate the biochemical processes leading to this detoxification strategy, the cell free extract of the control and the multiple-metal stressed cells were analyzed by HPLC. Disparate metabolite profiles were observed with an oxalate peak markedly higher in the stressed cells compared to the control cells. The latter soluble fraction had elevated levels of isocitrate and succinate (Fig. 1B). The analysis of select enzymes of the TCA cycle and electron-transport chain (ETC) by BN-PAGE activity assays revealed marked change in numerous enzymes. The activity of complex IV and ICDH-NAD was barely evident in the stressed cells (Fig. 2A). There was also a significant reduction in the activities of complex I, αKGDH and MDH (Fig. 2B). Isocitrate lyase (ICL), an enzyme that produces glyoxylate and succinic acid was increased in the cells grown in the multiple-metal medium (Fig. 2C). This diminution in NADH-producing enzymes and enzymes involved in the ETC was coupled to the increase in NADPH-forming enzymes. Malic enzyme and ICDH-NADP were characterized by an increase in activities in the stressed cells (Fig. 2D). Indeed, NAD and NADH production was lowered in the metal-treated cells, while NADP and NADPH production was up-regulated (Fig. 2E, F). Select enzymes were monitored by spectrophotometric assays to confirm the findings from in-gel activity assays. In particular, NADH and NADPH-producing enzymes were verified, as well as AGODH for its contribution to oxalate homeostasis. Pyruvate carboxylase was used as an internal control, as this enzyme does not vary significantly in activity (Table 1).

The pellet involved in the sequestration of the metals contained oxalate as did the spent fluid (Fig. 3A). Since we have previously demonstrated that glyoxylate is an important precursor to oxalate production in Al-stressed cells (Hamel and Appanna, 2001), the soluble CFE was incubated with glyoxylate in an effort to monitor the formation of the dicarboxylic acid. Indeed, the soluble CFE from the multiple metal-stressed cells readily generated oxalate and ATP (Fig. 3B). To elucidate the nature of this reaction, enzyme activity was evaluated by BN-PAGE. An activity band attributed to acylating glyoxylate dehydrogenase was observed in the stressed bacteria (Fig. 3C). This enzyme readily utilized $NADP^+$ as a co-factor rather than NAD^+. It was important to understand how ATP was being generated in the multiple metal-stressed cultures since the ETC was sharply diminished. The production of ATP was evident only in the stressed bacteria when the CFE was incubated with KCN, an inhibitor of complex IV, citrate and ADP (Fig. 4 A). This

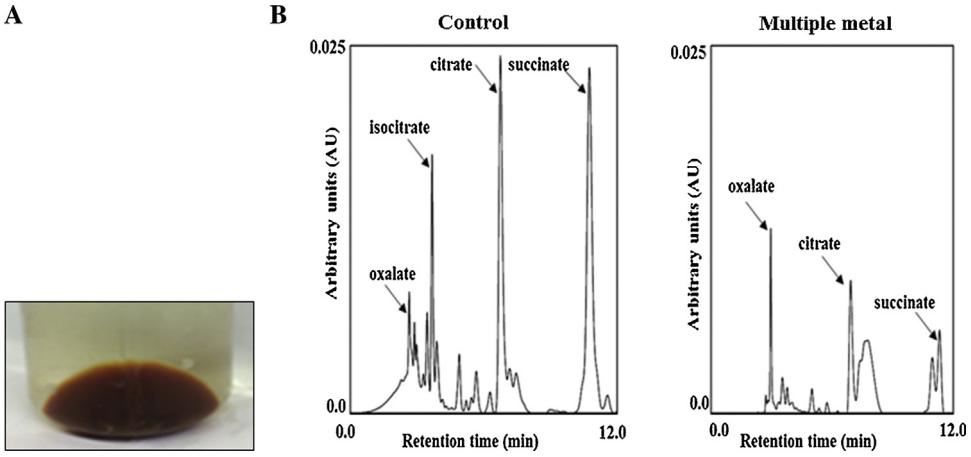

Fig. 1. Profiling metabolites from soluble cell free extract from control and multiple metal-stressed cultures. (A) Photograph of the gelatinous pellet from the metal-stressed culture (note the brown gelatinous residue). (B) Metabolite profiles in the soluble cell free extracts from the control and multiple metal-stressed cultures (Representative chromatogram; $n = 3$).

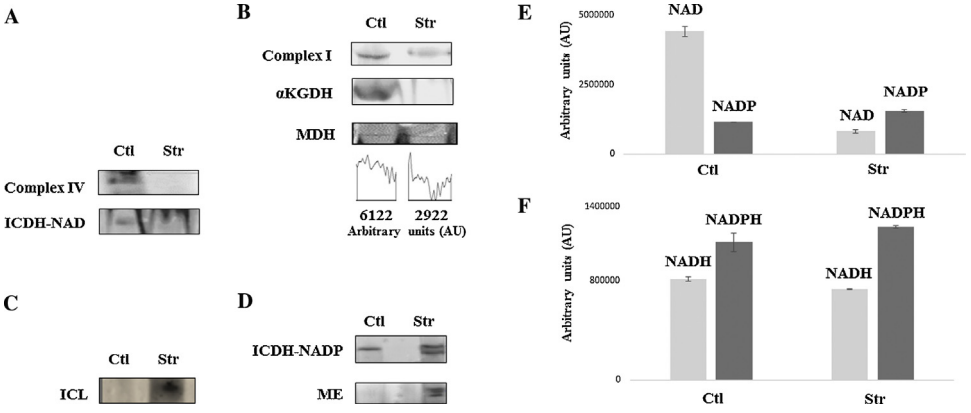

Fig. 2. Effect of multiple-metal stress on the TCA cycle and oxidative phosphorylation enzymes as visualized by BN-PAGE. (A) In-gel activity of complex IV and ICDH-NAD. (B) In-gel activity of complex I, αKGDH and MDH. Densitometry was performed using ImageJ for Windows. (C) In-gel activity of ICL. (D) In-gel activity of ICDH-NADP and ME. Cells were obtained at the same growth phase. Gels are representative of 3 independent experiments. (E) Oxidized nicotinamide adenine dinucleotide concentrations as measured by HPLC. (F) Reduced nicotinamide adenine dinucleotide concentrations as measured by HPLC. Ctl = Control; Str = Multiple metal treatment.

Table 1
Various enzymatic activities in cell-free extracts from control and stressed bacteria at the same growth phase as monitored via spectrophotometry.

Enzyme name	Control	Multiple metal-treated
NAD+-dependent isocitrate dehydrogenase[a]	0.96 ± 0.07	0.27 ± 0.06
Malate dehydrogenase[a]	0.43 ± 0.02	0.26 ± 0.03
Pyruvate carboxylase[b]	1.24 ± 0.09	1.19 ± 0.11
NADP+-dependent isocitrate dehydrogenase[c]	0.606 ± 0.04	0.908 ± .04
Malic enzyme[c]	0.45 ± .021	0.581 ± 0.15
Acylating glyoxylate dehydrogenase[c]	0.205 ± 0.02	0.25 ± 0.009

[a] μmol NADH produced min^{-1} mg $protein^{-1}$ as monitored at 340 nm ($n = 3 \pm$ standard deviation).
[b] μmol NADH consumed min^{-1} mg $protein^{-1}$ as monitored at 340 nm ($n = 3 \pm$ standard deviation).
[c] μmol NADPH produced min^{-1} mg $protein^{-1}$ as monitored at 340 nm ($n = 3 \pm$ standard deviation).

indicated that under the challenge of a multiple-metal stress, the microbe was fulfilling its energy requirement via substrate level phosphorylation instead of oxidative phosphorylation.

The foregoing data point to the ability of *Pseudomonas fluorescens* to survive a multi-metal environment by elaborating an intricate metabolic shift aimed at producing NADPH and oxalate coupled to the reduction in the synthesis of NADH, a pro-oxidant. The formation of ATP is promoted via substrate-level phosphorylation as oxidative phosphorylation is ineffective. These metabolic networks operate in tandem in an effort to optimize this detoxification strategy. The immobilization of Al is coupled to a reduction in the synthesis of the pro-oxidant NADH and increase in the formation of the anti-oxidant NADPH. The toxicity of Al and Ga is associated with the perturbation of Fe-metabolism as these toxicants can be readily incorporated in Fe-containing protein (Cornelis, 2008; Kaneko et al., 2007). This situation is punctuated by an increase in reactive oxygen species (ROS) and the inability of Fe-containing enzymes to function effectively (Halliwell, 2006; Yamamoto et al., 2002). Zn and Fe imbalance would also trigger a similar oxidative situation (Alhasawi et al., 2014).

To help alleviate the oxidative burden, *Pseudomonas fluorescens* down-regulated the activities of enzymes involved in the formation of the pro-oxidant NADH; hence, there is a marked reduction in enzymes like ICDH-NAD and αKGDH. Furthermore, the ETC that usually leads to the leakage of e^-, a factor contributing to oxidative stress was also reduced. To promote an intracellular anti-oxidative environment, NADPH-generating enzymes like ICDH-NADP and ME underwent a sharp increase. The presence of multiple bands pointed to isozymes in the stressed cells. The modulation of NADH and NADPH homeostasis is known to be finely-tuned in response to oxidative stress (Ying, 2008; Rui et al., 2010). We have also recently shown the role of NADK in mitigating the influence of ROS by shifting the metabolic flux toward NADPH formation. The role of catalase, superoxide dismutase and αKG has also been observed previously (Mailloux et al., 2007, 2011). Although this metabolic reconfiguration would help in neutralizing the impact of the multi-metal stress, it is critical that an organism has to immobilize these metals as innocuous moieties in order to quell their toxic impact. When organisms have to deal with these metals separately, they have been shown to elaborate intricate detoxification strategies dedicated to each metal. Zn can be immobilized intracellularly as a derivative of metallothioneins, and may also be precipitated as ZnS (Radhika et al., 2006). $CaCO_3$ acts as an excellent depository

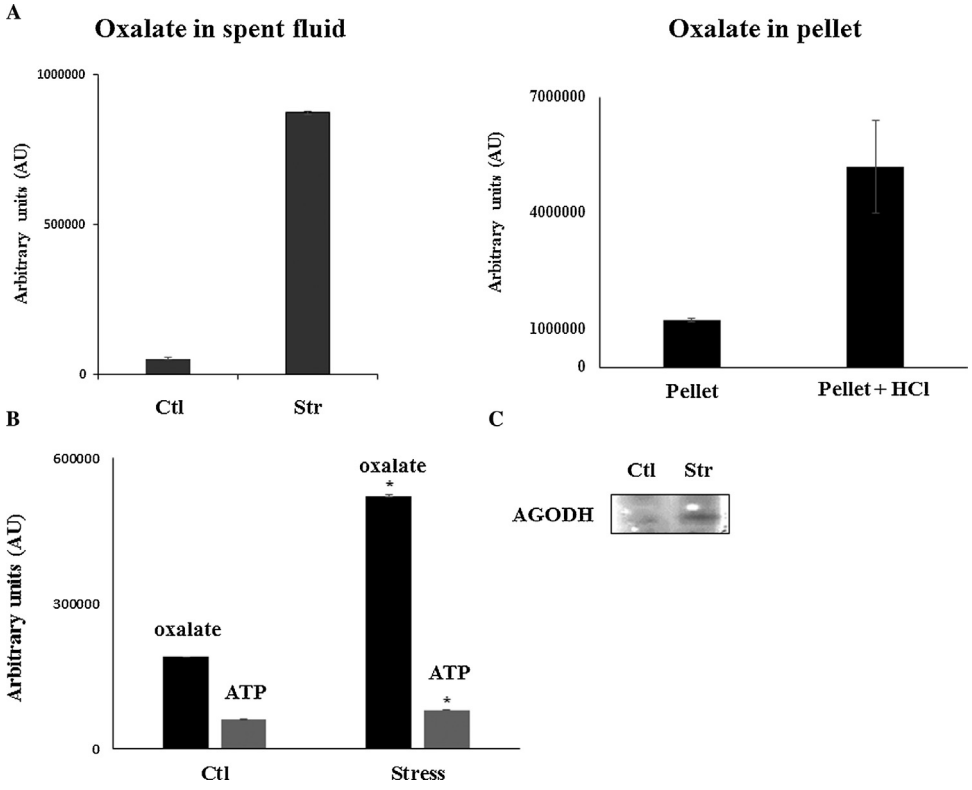

Fig. 3. Oxalate as a metal chelating agent. (A) Oxalate was measured by HPLC in the spent fluid of control (Ctl) and multiple metal-treated (Str) cultures as well as the gelatinous pellet of metal-stressed *P. fluorescens*. HCl was added to release oxalate prior to HPLC analysis. (B) Oxalate (■) and ATP (■) formation in soluble CFE treated with 2 mM glyoxylate, 2 mM succinate and 0.5 mM ADP for 30 min. Reactions were halted by boiling the solutions and metabolites were subjected to HPLC analysis. (C) In-gel activity staining of AGODH. Ctl = Control; Str = Multiple metal treatment. Cells were obtained at same growth phase; $n = 3 \pm$ SD; (*) Denotes a statistically significant difference compared to control ($p \leq 0.05$).

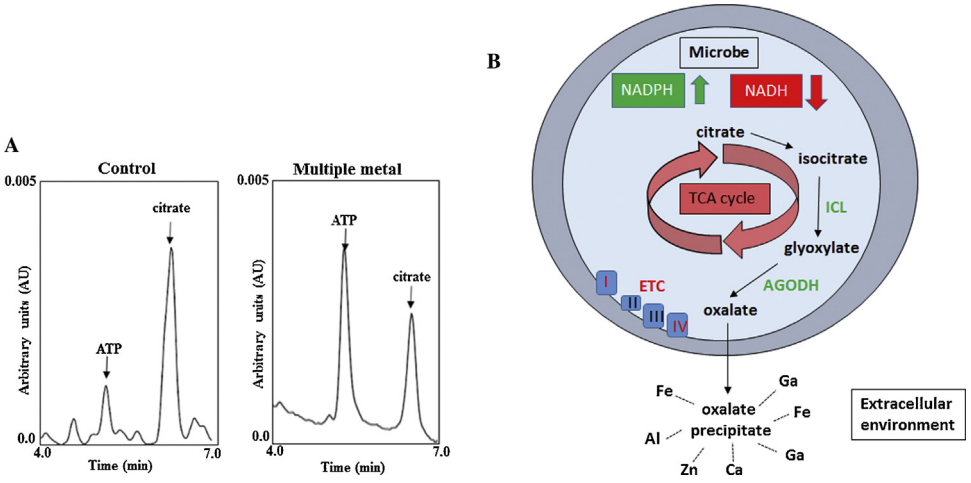

Fig. 4. ATP formation and metabolic adaptation in multiple metal-treated *P. fluorescens*. (A) Cell free extracts from control and multiple metal-treated bacteria at the same growth phase were incubated with 5 mM KCN, 2 mM citrate and 0.5 mM ADP for 30 min. Reactions were halted by boiling the solutions. ATP and citrate levels were gauged by HPLC analysis (representative chromatograms; $n = 3$). (B) Schematic demonstrating the metabolic shift in multiple metal-treated *P. fluorescens* leading to the production of oxalate and ATP via the glyoxylate shunt (ETC: electron-transport chain; ICL: isocitrate lyase; AGODH: acylating glyoxylate dehydrogenase).

for Ca and Ca efflux pumps helps maintain Ca levels at physiological concentration (Cacchio et al., 2012; Martel and Young, 2008). The ability of Ga to mimic Fe renders this trivalent metal very toxic. Indeed, Ga has been proposed as a potent antibiotic and is clinically utilized to detect rapidly dividing cancer cells as the need for Fe compels these cells to accumulate Ga (Auger et al., 2012; Jakupec and Keppler, 2004). *Pseudomonas fluorescens* has been shown to survive millimolar amounts of Ga by elaborating a hydroxyaspartate-derived chelator (Beriault et al., 2007). Al, another Fe mimetic is known to trigger the production of phosphatidylethanolamine and oxalate. These moieties act in tandem to immobilize the metal and deposit it extracellularly as insoluble precipitate (Hamel and Appanna, 2003). Some microbes do also utilize ATP-dependent pumps to efflux Al and its sequestration in the microbial outer membrane has been demonstrated (Amaral et al., 2013; Ferguson and Deisenhofer, 2004). There are relatively few studies on the ability of living systems to adapt to a multi-metal stress. The toxicity of multiple metals may have an additive effect and, or the presence of disparate metals may help mitigate the negative influence of some of the more toxic metals. For instance, the presence of micromolar amounts of Fe has been reported to reverse the toxicity of Ga (Al-Aoukaty et al., 1992; Auger et al., 2013). However, in this instance due to the elevated levels of all five metals, it is unlikely such a mitigating impact would be evident. Indeed, all these metals, when present individually, evoke a tailor-made detoxification response. Even, an essential element like Fe^{3+} is eliminated as an insoluble residue (Appanna and Finn, 1995). It appears that *Pseudomonas fluorescens* opts for a strategy to collectively neutralize all the metals rather than elaborate disparate pathways aimed at each metal. This mechanism may be less energy-demanding and easier to modulate. The ability of oxalate to bind to all these metals makes this dicarboxylic acid an ideal tool to sequester the metals (Gadd, 2010; Jáuregui-Zúñiga et al., 2005). Furthermore, its synthesis mediated by acylating glyoxylate dehydrogenase also provides a critical route to NADPH and ATP, two pivotal ingredients for the survival of the microbe.

4. Conclusion

The metabolic networks evoked by *Pseudomonas fluorescens* operate in tandem to generate oxalate, NADPH and ATP. These moieties ensure the survival of the organism by enabling the sequestration of all five disparate metals, promoting an anti-oxidative environment and generating ATP independent of O_2 (Fig. 4B). These molecular findings may help devise technologies aimed at remediating environments polluted with multiple metals, a situation common in nature.

Acknowledgments

This work was supported by Laurentian University and Industry Canada. Azhar Alhasawi is a recipient of funding from the Ministry of Higher Education of Saudi Arabia.

References

Rajapaksha, R., Tobor-Kapłon, M.A., Bååth, E., 2004. Metal toxicity affects fungal and bacterial activities in soil differently. Appl. Environ. Microbiol. 70, 2966–2973.
Lemire, J., Mailloux, R., Auger, C., Whalen, D., Appanna, V.D., 2010a. Pseudomonas fluorescens orchestrates a fine metabolic-balancing act to counter aluminium toxicity. Environ. Microbiol. 12, 1384–1390.
Alhasawi, A., Auger, C., Appanna, V.P., Chahma, M., Appanna, V.D., 2014. Zinc toxicity and ATP production in *Pseudomonas fluorescens*. J. Appl. Microbiol. 117, 65–73.
Wingfield, J.C., Kelley, J.P., Angelier, F., 2011. What are extreme environmental conditions and how do organisms cope with them. Curr. Zool. 57, 363–374.
Clemens, S., 2001. Molecular mechanism of plant metal tolerance and homeostasis. Planta 212, 475–486.
Hall, J.L., 2002. Cellular mechanisms for heavy metal detoxification and tolerance. J. Exp. Bot. 53, 1–11.
Appanna, V.D., Hamel, R., 1996. Aluminum detoxification mechanism in *Pseudomonas fluorescens* is dependent on iron. FEMS Microbiol. Lett. 143, 223–228.
Song, X., Van Heyst, B., 2005. Volatilization of mercury from soils in response to simulated precipitation. Atmos. Environ. 39, 7494–7505.
Adeyemi, A.O., 2010. Biological Immobilization of lead from lead sulphide by *Aspergillus Niger* and *Serpula Himantioidesl*. Int. J. Environ. Res. 3, 477–482.
Anderson, S., Appanna, V.D., Huang, J., Viswanatha, T., 1992. A novel role for calcite in calcium homeostasis. FEBS Lett. 308, 94–96.
Blindauer, C.A., Harrison, M.D., Robinson, A.K., Parkinson, J.A., Bowness, P.W., Sadler, P.J., Robinson, N.J., 2002. Multiple bacteria encode metallothioneins and SmtA-like zinc fingers. Mol. Microbiol. 45, 1421–1432.
Reinoso, C.A., Auger, C., Appanna, V.D., Vásquez, C.C., 2012. Tellurite-exposed *Escherichia coli* exhibits increased intracellular α-ketoglutarate. Biochem. Biophys. Res. Commun. 421, 721–726.
Reinoso, C.A., Appanna, V.D., Vásquez, C.C., 2013. α-Ketoglutarate accumulation is not dependent on isocitrate dehydrogenase activity during tellurite detoxification in *Escherichia coli*. BioMed. Res. Int. 2013, 1–7.
Appanna, V.D., St Pierre, M., 1996. Cellular response to a multiple-metal stress in *Pseudomonas fluorescens*. J. Biotech. 48, 129–136.
Singh, R., Chenier, D., Beriault, R., Mailloux, R., Hamel, R.D., Appanna, V.D., 2005. Blue native polyacrylamide gel electrophoresis and the monitoring of malate-and oxaloacetate-producing enzymes. J. Biochem. Biophys. Met. 64, 189–199.
Bradford, M.M., 1976. A rapid and sensitive method for the quantitation of microgram quantities of protein utilizing the principle of protein-dye binding. Anal. Biochem. 72, 248–254.

Singh, R., Mailloux, R.J., Puiseux-Dao, S., Appanna, V.D., 2007. Oxidative stress evokes a metabolic adaptation that favors increased NADPH synthesis and decreased NADH production in *Pseudomonas fluorescens*. J. Bacteriol. 189, 6665–6675.

Lemire, J., Milandu, Y., Auger, C., Bignucolo, A., Appanna, V.P., Appanna, V.D., 2010b. Histidine is a source of the antioxidant, a-ketoglutarate, in *Pseudomonas fluorescens* challenged by oxidative stress. FEMS Microbiol. Lett. 309, 170–177.

Auger, C., Appanna, V., Castonguay, Z., Han, S., Appanna, V.D., 2012. A facile electrophoretic technique to monitor phosphoenolpyruvate-dependent kinases. Electrophoresis 33, 1095–1101.

Han, S., Auger, C., Castonguay, Z., Appanna, V.P., Thomas, S.C., Appanna, V.D., 2013. The unravelling of metabolic dysfunctions linked to metal-associated diseases by blue native polyacrylamide gel electrophoresis. Anal. Bioanal. Chem. 405, 1821–1831.

Hamel, R.D., Appanna, V.D., 2001. Modulation of TCA cycle enzymes and aluminum stress in *Pseudomonas fluorescens*. J. Inorg. Biochem. 87, 1–8.

Cornelis, P., 2008. Unexpected interaction of a siderophore with aluminum and its receptor. J. Bac. 190, 6541–6543.

Kaneko, Y., Thoendel, M., Olakanmi, O., Britigan, B.E., Singh, P.K., 2007. The transition metal gallium disrupts *Pseudomonas aeruginosa* iron metabolism and has antimicrobial and antibiofilm activity. J. Clin. Invest. 117, 877–888.

Halliwell, B., 2006. Reactive species and antioxidants. Redox biology is a fundamental theme of aerobic life. Plant Physiol. 141, 312–322.

Yamamoto, Y., Kobayashi, Y., Devi, S.R., Rikiishi, S., Matsumoto, H., 2002. Aluminum toxicity is associated with mitochondrial dysfunction and the production of reactive oxygen species in plant cells. Plant Physiol. 128, 63–72.

Ying, W., 2008. NAD^+/NADH and $NADP^+$/NADPH in cellular functions and cell death: regulation and biological consequences. Antioxid. Redox Signal. 10, 179–206.

Rui, B., Shen, T., Zhou, H., Liu, J., Chen, J., Pan, X., Shi, Y., 2010. A systematic investigation of *Escherichia coli* central carbon metabolism in response to superoxide stress. BMC Syst. Biol. 4, 122.

Mailloux, R.J., Bériault, R., Lemire, J., Singh, R., Chénier, D.R., Hamel, R.D., Appanna, V.D., 2007. The tricarboxylic acid cycle, an ancient metabolic network with a novel twist. PLoS One 2, e690.

Mailloux, R.J., Lemire, J., Appanna, V.D., 2011. Metabolic networks to combat oxidative stress in *Pseudomonas fluorescens*. Antonie van Leeuwenhoek 99, 433–442.

Radhika, V., Subramanian, S., Natarajan, K.A., 2006. Bioremediation of zinc using *Desulfotomaculum nigrificans:* Bioprecipitation and characterization studies. Water Res. 40, 3628–3636.

Cacchio, P., Ercole, C.L., Contento, R., Cappuccio, G., Martinez, M.P., Del Gallc, M., Lepidi, A.L., 2012. Involvement of bacteria in the origin of newly described speleothem in the gypsum cave of grave (Crotone, Italy). J. Cave Karst. Stud. 74, 7–18.

Martel, J., Young, J.D., 2008. Purported nanobacteria in human blood as calcium carbonate nanoparticles. Proc. Natl. Acad. Sci. U.S.A. 105, 5549–5554.

Jakupec, M.A., Keppler, B.K., 2004. Gallium in cancer treatment. Curr. Top. Med. Chem. 4, 1575–1583.

Beriault, R., Hamel, R., Chenier, D., Mailloux, R.J., Joly, H., Appanna, V.D., 2007. The overexpression of NADPH-producing enzymes counters the oxidative stress evoked by gallium, an iron mimetic. Biometals 20, 165–176.

Hamel, R., Appanna, V.D., 2003. Aluminum detoxification in *Pseudomonas fluorescens* is mediated by oxalate and phosphatidylethanolamine. Biochim. Biophys. Acta 1619, 70–76.

Amaral, L., Martins, A., Spengler, G., Molnar, J., 2013. Efflux pumps of Gram-negative bacteria: what they do, how they do it, with what and how to deal with them. Front. Pharmacol. 4, 1–11.

Ferguson, A.D., Deisenhofer, J., 2004. Metal import through microbial membranes. Cell 116, 15–24.

Al-Aoukaty, A., Appanna, V.D., Falter, H., 1992. Gallium toxicity and adaptation in *Pseudomonas fluorescens*. FEMS Microbiol. Lett. 92, 265–272.

Auger, C., Lemire, J., Appanna, V.P., Appanna, V.D., 2013. Gallium in Bacteria, Metabolic and Medical Implications. Encyclopedia of Metalloproteins. Springer, pp. 800–807.

Appanna, V.D., Finn, H., 1995. Microbial adaptation to iron: a possible role of phosphatidylethanolamine in iron mineral deposition. Biometals 8, 142–148.

Gadd, G.M., 2010. Metals, minerals and microbes: geomicrobiology and bioremediation. Microbiol. 156, 609–643.

Jáuregui-Zúñiga, D., Ferrer, A., Calderón, A.A., Muñoz, R., Moreno, A., 2005. Heavy metal stress reduces the deposition of calcium oxalate crystals in leaves of *Phaseolus vulgaris*. J. Plant Physiol. 162, 1183–1187.